

# Morphological complexities and hazards during the emplacement of channel-fed 'a'ā lava flow fields: A study of the 2001 lower flow field on Etna

L. J. Applegarth · H. Pinkerton · M. R. James · S. Calvari

Received: 19 August 2009 / Accepted: 20 January 2010 / Published online: 17 February 2010  
© Springer-Verlag 2010

**Abstract** Long-lived basaltic eruptions often produce structurally complex, compound 'a'ā flow fields. Here we reconstruct the development of a compound flow field emplaced during the 2001 eruption of Mt. Etna (Italy). Following an initial phase of cooling-limited advance, the reactivation of stationary flows by superposition of new units caused significant channel drainage. Later, blockages in the channel and effusion rate variations resulted in breaching events that produced two new major flow branches. We also examined small-scale, late-stage 'squeeze-up' extrusions that were widespread in the flow field. We classified these as 'flows', 'tumuli' or 'spines' on the basis of their morphology, which depended on the rheology, extrusion rate and cooling history of the lava. Squeeze-up flows were produced when the lava was fluid enough to drain away from the source bocca, but fragmented to produce blade-like features that differed markedly from 'a'ā clinker. As activity waned, increased cooling and degassing led to lava arriving at boccas with a higher yield strength. In many cases this was unable to flow after extrusion, and laterally extensive, near-vertical sheets of

lava developed. These are considered to be exogenous forms of tumuli. In the highest yield strength cases, near-solid lava was extruded from the flow core as a result of ramping, forming spines. The morphology and location of the squeeze-ups provides insight into the flow rheology at the time of their formation. Because they represent the final stages of activity of the flow, they may also help to refine estimates of the most advanced rheological states in which lava can be considered to flow. Our observations suggest that real-time monitoring of compound flow field evolution may allow complex processes such as channel breaching and bocca formation to be forecast. In addition, documenting the occurrence and morphology of squeeze-ups may allow us to determine whether there is any risk of a stalled flow front being reactivated. This will therefore enhance our ability to track and assess hazard posed by lava flow emplacement.

**Keywords** Basaltic 'a'ā · Channel-fed lava · Effusion rate · Squeeze-up · Tumuli · Etna

Editorial responsibility: A. Harris

**Electronic supplementary material** The online version of this article (doi:10.1007/s00445-010-0351-1) contains supplementary material, which is available to authorized users.

L. J. Applegarth (✉) · H. Pinkerton · M. R. James  
Lancaster Environment Centre, Lancaster University,  
Bailrigg,  
Lancaster LA1 4YQ, UK  
e-mail: l.j.applegarth@lancaster.ac.uk

S. Calvari  
Sezione di Catania,  
Istituto Nazionale di Geofisica e Vulcanologia,  
Piazza Roma 2,  
95125 Catania, Italy

## Introduction

Considerable advances in lava flow modelling over the past decade mean that it is now possible to estimate the final lengths and inundation areas of single flow units (e.g. Calvari and Pinkerton 1998; Harris and Rowland 2001; Favalli et al. 2005; Wright et al. 2008), and to replicate their emplacement using cellular automata models (e.g. Crisci et al. 2004; Hidaka et al. 2005; Vicari et al. 2007). However, during basaltic eruptions it is common for activity to persist beyond the time taken for individual units to reach their cooling-limited lengths. New flow units are therefore emplaced alongside and on top of earlier units, resulting in compound flow fields. On Mt. Etna (Sicily, Italy), these

are often dominated by 'a'ā surface textures (Chester et al. 1985; Kilburn 1990). Fluctuations in effusion rate also contribute to increasing structural complexity (e.g. Frazzetta and Romano 1984; Guest et al. 1987; Calvari et al. 2003). To improve our understanding of the development of compound flow fields, it is necessary to study them in detail both during and after emplacement.

The 2001 flank eruption of Etna provided an excellent opportunity to examine the large-scale structural evolution of a compound flow field, and the complex surface features that are widespread in many 'a'ā flows. The eruption involved activity at seven effusive vents on two fissure systems between July 17th and August 9th (Calvari and INGV Catania staff 2001; Behncke and Neri 2003; Calvari and Pinkerton 2004). The resultant flow fields are shown in Fig. 1. The upper fissure system was host to five vents above 2,600 m elevation, on an approximately north-south transect east of the summit craters. The lower fissure system fed two vents on the southern flank, at 2,550 m and 2,100 m above

sea level (a.s.l.) (Fig. 1). The 2,100 m vent, to the north east of the Sapienza tourist complex, was active between July 18th and August 9th, and produced the largest lava flow field of the eruption. This flow field is the subject of our study and is hereafter referred to as the 'lower flow field'. The lower flow field reached its maximum length of 6.4 km in 8 days, after which time new flow units were emplaced as overflows from the original channel, or surface flows overlying earlier units within the channel (Behncke and Neri 2003; Coltelli et al. 2007; Favalli et al. 2010). Two new major flow branches later developed as a result of channel breaching. The most prominent aspects of the post-eruption structure are shown in Fig. 2, and a detailed map is provided as Online Resource 1.

The eruption was monitored closely by the staff of the Istituto Nazionale di Geofisica e Vulcanologia (INGV), Catania, who collected visible images during several helicopter overflights, and published daily reports of activity online (Istituto Nazionale di Geofisica e Vulcanologia (Catania) syn-eruption reports: <http://www.ct.ingv.it/Etna2001/Main.htm>). We have used these data together with thermal images and video footage collected between July 26th and August 4th, post-eruption aerial photos and field observations to unravel the structural and temporal evolution of the lower flow field.

The advance and development of the flow before July 26th, when it reached its maximum length, has been described elsewhere (e.g. Calvari and INGV Catania staff 2001; Behncke and Neri 2003; Coltelli et al. 2007). More detailed morphological analysis was carried out by Favalli et al. (2010), who mapped the distal 1.5 km of the flow field with metre precision using LIDAR data collected in 2004–5 (Mazzarini et al. 2005). Their work examined the mechanisms of flow advance, and of and levée and channel formation.

Here we concentrate on developments throughout the lower flow field after July 26th, examining the processes that resulted in the highly complex final structure (Fig. 2). From this analysis, we are able to reconstruct the late-stage growth of the flow field, including the emplacement and inflation of new flow units, the formation of ephemeral boccas, the development of subsurface thermal pathways, the initiation of new flows through levée breaching, and the drainage of flow units and channels. We also consider the role of effusion rate fluctuations in these late-stage changes.

Of interest on a smaller scale is the widespread occurrence of late-stage 'squeeze-ups' of lava, in a range of rheological states, through flow surfaces and around flow margins. These are inferred to have developed on stationary flow units, which were reactivated following changes in the prevailing flow conditions (Applegarth 2008).

The following section details aspects of the overall structural development of the lower flow field. We then reduce the spatial scale of our observations, looking first at processes within one short flow sector, before focussing on post-emplacement changes in the flow field.

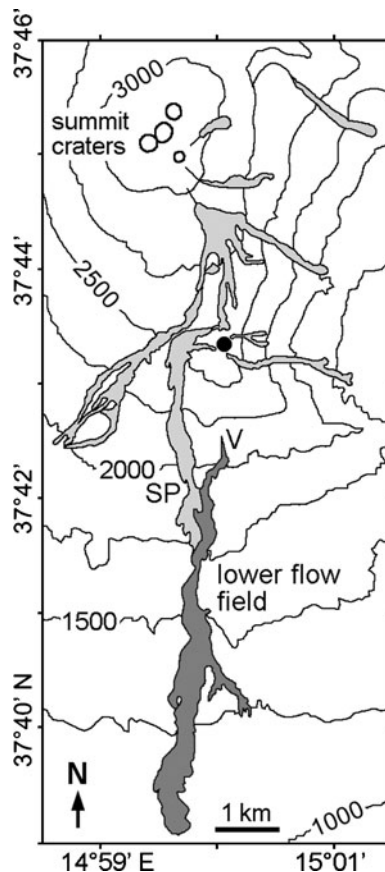
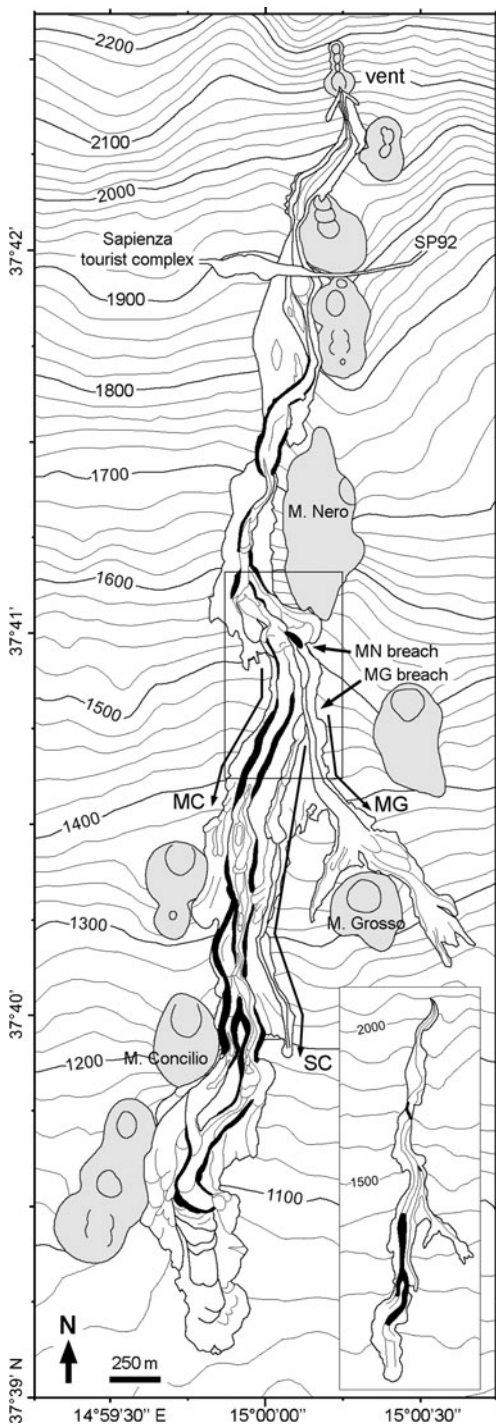


**Fig. 1** Sketch map showing the flows emplaced during the 2001 Etna eruption. All flows emplaced during the 2001 eruption are shaded, with *darker grey* representing the lower flow field. The 2,100 m vent is labelled 'V', and the filled *black circle* shows the location of the cinder cone that grew during magmatic activity at the 2,550 m vent. 'SP' indicates the location of the Sapienza tourist complex. Contour interval is 250 m



**Large-scale flow field development**

**Eruption chronology**

The early development of the lower flow field (July 18th–31st) is well documented in the syn-eruption reports of INGV (<http://www.ct.ingv.it/Etna2001/Main.htm>), and in Behncke and Neri (2003) and Coltelli et al. (2007). Details

**Fig. 2** Sketch map showing the post-eruption structure of the lower flow field. SP92 is the Nicolosi-Sapienza-Zafferana road that cuts through the proximal part of the flow field. Historic cinder cones are shown in grey, and those referred to in the text are named. The three principal channels are labelled. MC is the main channel, and extends from the vent down the western side of the flow field to the flow front. SC is the secondary channel, and MG is the Monte Grosso channel, which bifurcates around the Monte Grosso cinder cone. Arrows show the initial direction of the paths taken by the three channels below Monte Nero, where SC and MG originate. High relief levées are shown in black. The Monte Nero (MN) breach is where the secondary channel broke out from the main channel, and the Monte Grosso (MG) breach where the Monte Grosso channel broke out from the secondary channel (Fig. 4). Inset shows drained channels in black. Box shows the flow sector examined in detail in Fig. 5

of the advance and evolution of the flow front between July 20th and August 2nd can be found in Favalli et al. (2010). We begin with a brief description of some of the features that formed during this period, and then move on to document significant events in flow field development after July 31st.

The 2,100 m vent opened in the early hours of July 18th and fed a lava flow that formed a well-defined channel within the first few hours of activity. This continued to advance as a single channel-fed flow until reaching its maximum length on July 26th (Behncke and Neri 2003; Coltelli et al. 2007; Favalli et al. 2010) (Fig. 3). The decreasing advance rate of the flow front (Fig. 3) and the presence of surface flows and overflows behind the front before July 26th (INGV internal report 24/07/01) suggest

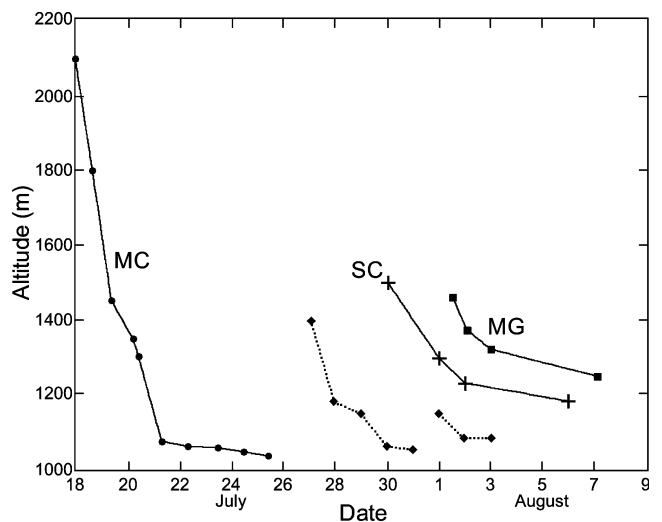


**Fig. 3** Plot showing the advance of the lower flow field by active flow front altitude as a function of time. The main, secondary and Monte Grosso channels (MC, SC and MG respectively) show cooling-limited advance trends. The dotted curves show the progression of new surface flow units in the main channel after the flow field reached its maximum length. The data are from both INGV internal reports and our observations

that the main channel was cooling-limited. Following the cessation of flow front advance, the juxtaposition and superposition of new flow units behind the flow front led to widening and thickening of the flow field (Favalli et al. 2010). The onset of magmatic activity at the 2,550 m vent on July 26th caused a reduction in effusion rate at the 2,100 m vent, and hence diminished activity in the lower flow field (Behncke and Neri 2003; Calvari and Pinkerton 2004; Favalli et al. 2010).

As shown in Fig. 3, the most advanced active front in the lower flow field was overlying earlier flows at 1,400 m a.s.l. on July 27th (INGV internal report 27/07/01). By July 28th the active flows had reached 1,180 m a.s.l. (Coltelli et al. 2007). This rapid advance is thought to have resulted from the reactivation of the earlier flows by the overlying unit, which caused substantial drainage of the main channel between 1,400 and 1,100 m a.s.l. (Fig. 2, inset). This process explains why the apparently cooling-limited main channel is drained in this region, when drainage is more

usually associated with volume-limited flows (Borgia et al. 1983; Pinkerton and Wilson 1994). After the drainage event, an ephemeral bocca was active in the channel at 1,400 m a.s.l. until August 12th, indicating subsurface flow within the channel immediately upslope.

On July 30th breaching of the main channel at ~1,500 m a.s.l. (below Monte Nero) led to a new flow that advanced to the south, parallel to the eastern margin of the flow field (Coltelli et al. 2007). We call this new flow the secondary channel (Figs. 2, 4a). When magmatic activity ceased at the 2,550 m vent on August 1st, a transient increase in effusion rate was observed at the 2,100 m vent (Behncke and Neri 2003). Thermal images from this date show that the main and secondary channels contained several ephemeral boccas, and that the most advanced active flow in the main channel consisted of two arms below 1,250 m a.s.l. (Favalli et al. 2010) (Fig. 4a). The active fronts were not as advanced on August 1st as they had been at the end of July (INGV internal reports 31/07/01,

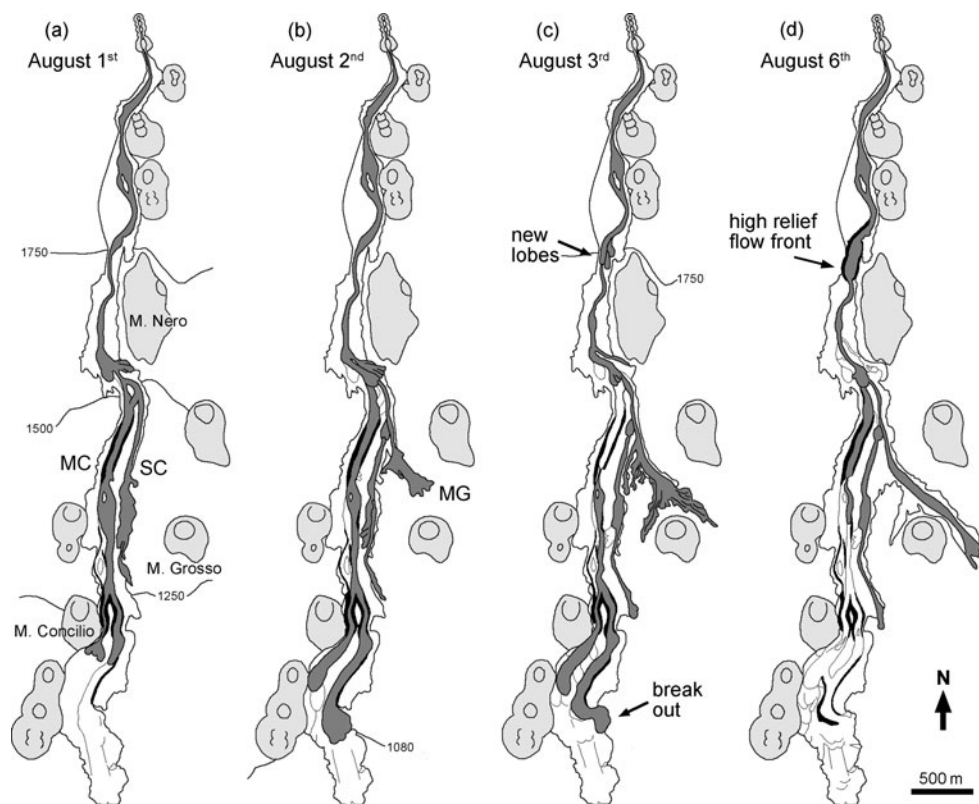


**Fig. 4** Sketches showing the development of the lower flow field between August 1st and 6th, with the active flows shown in *dark grey*. High relief levées are shown in *black*. Altitudes on contours are in metres. The activity on August 1st and 3rd is well constrained by thermal images, while that on August 2nd and 6th relies on visible images. **a** August 1st. The flow in the distal main channel (MC) is split into 2 arms at ~1,250 m a.s.l. The secondary channel (SC) is well established. **b** August 2nd. The Monte Grosso channel (MG) has initiated following a breakout from the secondary channel. Flows in

the main channel have advanced since August 1st. Position of the western front of the main channel flow is not well constrained. **c** August 3rd. A breakout has occurred to the east of the main channel at ~1,080 m a.s.l. Position of the western front of the main channel flow is not well constrained. New flow lobes overlying the main channel at 1,750 m a.s.l. are stagnating. **d** August 6th. Activity in the flow field is waning. The lobes noted in (c) have coalesced to form a wide, high-relief flow front that has been breached

01/08/01). This may be linked to the initiation of the secondary channel on July 30th, which could have diverted sufficient supply from the main channel so as to cause reduced activity in the distal flow field.

The eastern margin of the secondary channel was breached at ~1,450 m a.s.l. on August 2nd, producing a new flow that advanced to the south east (Coltelli et al. 2007) (Fig. 4b). This flow initially advanced as a sheet flow, but gradually became concentrated in a channel. We have named this new flow branch the Monte Grosso channel. Observations of the distal portion of the main channel on August 2nd showed that the two active fronts had advanced since August 1st (INGV internal report 02/08/01). This may have been due to the transient increase in effusion rate documented on that date. The eastern arm of the flow followed the original axis of the main channel, and had advanced to 1,080 m a.s.l. (Fig. 4b), while the shorter western arm was emplaced on top of earlier overflows from the channel (Favalli et al. 2010). Because the main channel was already full, the eastern arm built up above the height of the levées. Dust arising from rockfalls on the eastern levée is visible in images taken on August 2nd (Favalli et al. 2010), and the levee had failed by August 3rd to produce a breakout that advanced a few tens of metres (Fig. 4c).

By August 3rd, activity throughout the flow field was diminishing (Behncke and Neri 2003). This was illustrated by the presence of three new stagnating surface flow units overlying the main channel at 1,750 m a.s.l. ('new lobes' in Fig. 4c), which coalesced over the following few days to produce a wide, high relief flow front (Fig. 4d). This front was subsequently breached to allow the continued supply of lava to more distal parts of the flow field. After August 5th, the active part of the main channel narrowed significantly, evidenced by nested levées along the proximal 1,500 m (seen in the map in Online Resource 1). The secondary channel reached its maximum length on the 6th, while the Monte Grosso channel stopped advancing on the 7th having reached 1,240 m a.s.l. (Coltelli et al. 2007). Although activity at the vent ceased on the 9th, a few ephemeral boccas, including that at 1,400 m a.s.l., continued to feed small sluggish flows in the main channel until August 12th (INGV internal reports 9 to 12/08/01).

#### Effusion rates

The maximum cooling-limited length that a lava flow field can reach depends largely on the discharge rate (e.g. Walker 1973; Pinkerton and Wilson 1994; Calvari and Pinkerton 1998). However, small-scale changes in effusion rate on timescales of minutes to hours are known to significantly influence flow behaviour and morphology (e.g. Kauhikaua et al. 2003; Bailey et al. 2006; James et al. 2007).

Behncke and Neri (2003) and Coltelli et al. (2007) calculated time-averaged syn-eruption discharge rates (Harris et al. 2007) for the 2,100 m vent on a near-daily basis, using planimetric methods. These studies recorded an increase in the effusion rate over the first 5 to 6 days of activity, followed by a gradual decrease until the end of the eruption. Between July 26th and August 4th, one of us (Pinkerton) also observed the general trend of waning discharge rates, but recorded two notable exceptions in the form of short-lived increases in the effusion rate on July 31st and August 2nd. Neither these, nor the pulse reported on August 1st (Behncke and Neri 2003) were detected by the planimetric measurements because they were too small in volume and too short in duration. Despite the transient nature of the pulses, subsequent events, including the renewed advance of flow fronts in the distal portion of the main channel (Fig. 3) and the levée breach that led to the Monte Grosso channel on August 2nd, suggest that they had a significant effect on activity in the flow field.

#### Processes in the Monte Nero flow sector: Breaching, tube formation, squeeze-ups and drainage

Examining the evolution of the flow along a short section adjacent to Monte Nero (Fig. 2 (box), Fig. 5) allows us to gain a deeper understanding of the complex processes responsible for the final morphology of the lower flow field. Following the initiation of two new flows as a result of levée breaching, all three channels became increasingly stagnant in this region, developing subsurface supply pathways, ephemeral boccas, and late-stage squeeze-ups. We stress that the features discussed in this region are found throughout the flow field, which indicates that the processes responsible for their formation are common and repeatable.

When coupled with ongoing lava supply, the stagnation of a flow unit can result in inflation (possibly followed by breaching to form a bocca), the emplacement of overflows and/or surface flows, or breaching of the levée behind the blockage (Kilburn and Lopes 1988, 1991). All of these processes were observed in the lower flow field. Sustained lava supply through a breached front can represent the early stages of tube formation (Calvari and Pinkerton 1998), where 'tube' is specifically used to mean a subsurface lava pathway that could drain to leave a self-supporting roof. However, bocca formation does not always lead to tube formation, as steady lava supply is required for some period of time so that the roof can develop sufficient strength to become self-supporting (Calvari and Pinkerton 1998, 1999). Although subsurface pathways were widely observed in the lower flow field, they almost always caused significant surface deformation, and no unequivocal evidence of mature self-supporting tubes was seen. We

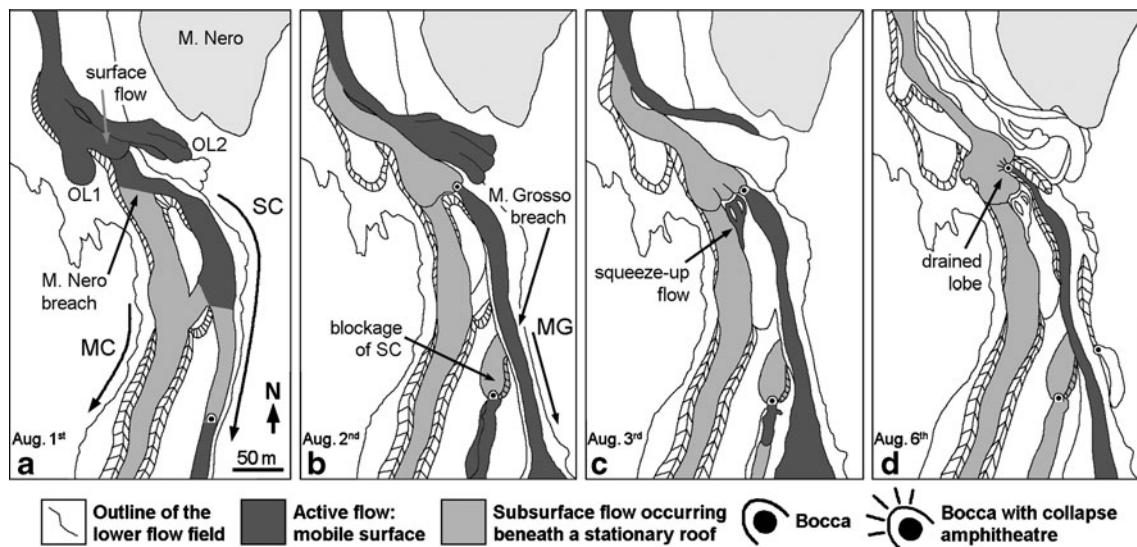


**Fig. 5** Sketches showing the development of the Monte Nero flow sector (box in Fig. 2) between August 1st and 6th. The Monte Nero cinder cone is shown in light grey. Mid grey indicates parts of the flow field which are active, but in which flow surfaces are stationary, while dark grey depicts active flow and a mobile flow surface. Hatching indicates high relief levées and flow fronts. **a** August 1st. A surface flow is advancing down the main channel (MC), while overflow lobes (OL1 & OL2) are emplaced to either side. The secondary channel (SC) is established, following the Monte Nero breaching event on July 30th. A thermal image from this date is shown in Fig. 6. **b** August

2nd. The surface flow has advanced to cover the breach site, and stagnated. A stationary front has developed in the secondary channel, and has failed, allowing continued supply to the channel below. Breaching of the secondary channel has occurred immediately upflow of the blockage, at the Monte Grosso breach site. The Monte Grosso channel (MG) is advancing south east. **c** August 3rd. High yield strength lava is being extruded through the flow margins between the main and secondary channels at the Monte Nero breach site. **d** The stationary surface flow emplaced on August 1st/2nd has been partly drained, resulting in a deep, wide amphitheatre (Fig. 7)

therefore prefer the term ‘thermal pathway’ to ‘tube’ in this context. Although this term is similar to the ‘thermally preferential pathway’ described by Guest and Stofan (2005) in their study of slab-crust flows on Etna, they use the expression to describe the phenomenon of lava injection beneath a stable (undeforming) but often moving crust. In contrast we are referring to a crust that is unstable (deforming) and is not moving down flow.

Although we did not observe the events leading to the Monte Nero breach on July 30th, we have examined those that led to the initiation of the Monte Grosso channel on August 2nd. On August 1st, a surface flow was observed advancing down the main channel above the Monte Nero breach site. Overflows had already occurred to either side of the channel in the same area (Fig. 5a). Thermal images indicate that the surfaces of these three new units were cool in comparison with the surface of the main channel immediately downflow (Fig. 6), suggesting that they were stagnating. Surface temperatures in the main channel below the Monte Nero breach were low, which supports our interpretation that a subsurface thermal pathway was active in this part of the main channel. That the roof of this pathway was being disrupted by the flow of lava beneath is evidenced by visible images showing that the surface of the main channel between the Monte Nero breach at 1,500 m and the bocca at 1,400 m was severely modified. Higher

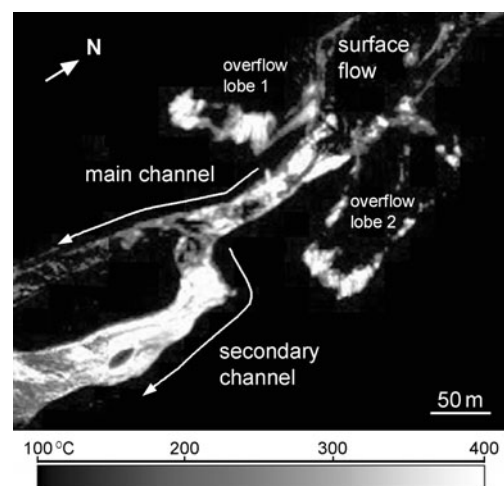


**Fig. 6** Thermal image of the Monte Nero breach site on August 1st, from the south east. The section of flow shown is approximately 500 m long. Greyscale bar shows apparent surface temperatures. The surface flow in the main channel can be seen, together with overflow lobes (1 & 2) to either side. The surfaces of these new units are cool compared to the surface of the main channel immediately below the surface flow lobe. Below the breach, the main channel surface temperature is again low, while that in the secondary channel remains high. Subsurface flow is therefore implied in the stagnating surface flow, and in the main channel below the breach, while open channel flow is occurring in the secondary channel

surface temperatures in the secondary channel (Fig. 6) suggest that open channel flow was occurring there on August 1st.

By August 2nd, the surface flow had advanced to overlie the Monte Nero breach site, and had come to rest abutting the south-western levée of the secondary channel (Fig. 5b). An arcuate collapse region had formed in the front of the surface flow, and degassing was observed in the secondary channel, indicating that supply to this channel was continuing from a bocca in the stationary flow front. Breaching of the eastern levée of the secondary channel further downslope had led to the initiation of the Monte Grosso channel, which was advancing in a direction  $\sim 40^\circ$  to the east of the flow field (Figs. 4b, 5b). Thermal and visible images acquired over the following days indicated that lava arriving at the Monte Grosso breach site was largely supplied to the new channel, and that activity in the secondary channel was waning.

Bocca development in the surface flow overlying the Monte Nero breach site is inferred to have been influenced by the underlying earlier flows. Dragoni and Tallarico (1996) modelled the opening of boccas in flow fronts assuming uniform crustal thicknesses and tensile strengths, and calculated that they should open preferentially at the base where the pressure is highest. Where a stationary unit overlies an earlier flow, the effect of higher pressure may be compounded by a thinner crust, due to reduced cooling at the base where the front is in contact with the underlying hot flow. In most cases, surface flows in the lower flow field were emplaced down the axes of earlier channels, and failure occurred in the approximate centre of the flow front. However, the surface flow that came to rest overlying the Monte Nero breach site experienced reduced cooling due to hot underlying flows in two distinct regions at its flow front (the main and secondary channels). Breaching could have occurred in either or both areas (Fig. 5b), but only did so in that part of the flow front that overlay the secondary channel. This may be because surface temperatures were higher in this channel than the main channel (Fig. 6), but was probably compounded by the fact that the secondary channel surface was still mobile, while the surface of the main channel adjacent to the Monte Nero breach was stationary.

The overflows on August 1st and the breaching event that initiated the Monte Grosso channel on August 2nd are thought to have resulted from the transient increases in effusion rate previously documented. In the case of the Monte Grosso breaching event, a high-relief stationary flow front had developed in the secondary channel at  $\sim 1,450$  m a.s.l. between August 1st and 2nd (Figs. 5a, b). Although a bocca had developed in this flow front so that supply to the secondary channel continued (Fig. 5b), the front presented a sufficient obstacle that the levée behind was

breached when the effusion rate increased briefly. Breaching of the main channel to initiate the secondary channel on July 30th may have resulted from a similar transient increase in effusion rate, though this was not recorded. Alternatively, it may have resulted from ponding of lava due to the effects of a blockage further down the channel, or a combination of the two. That ponding can cause levée failure was suggested by Favalli et al. (2010) in reference to the breakout behind the flow front on August 2nd/3rd (Fig. 4c), where the ponding occurred due to a break in slope.

On August 3rd, highly viscous lava was squeezed up through the margin of the secondary channel at the Monte Nero breach site (Fig. 5c). The squeeze-up reached approximately 50 m in length, and was much darker in colour and rougher in texture than the surrounding 'a'ā (Fig. 7). By August 6th, the part of the surface flow that had been overlying the secondary channel at the Monte Nero breach site had largely disappeared. This was due to continued drainage and collapse, which had formed a deep, steep-walled channel that ended upflow in an arcuate amphitheatre (Fig. 5d). The latest material to be emplaced in this channel was similar in colour and texture to the viscous extrusion of August 3rd (Fig. 7).

Our observations of the Monte Nero flow sector highlight the importance of stagnating flow units, subsurface thermal pathways, changes in effusion rate, breaching events, drainage and late-stage extrusions in determining the final flow field morphology. All of these features and processes are ubiquitous in the lower flow field. The significance of late-stage squeeze-ups, such as that extruded

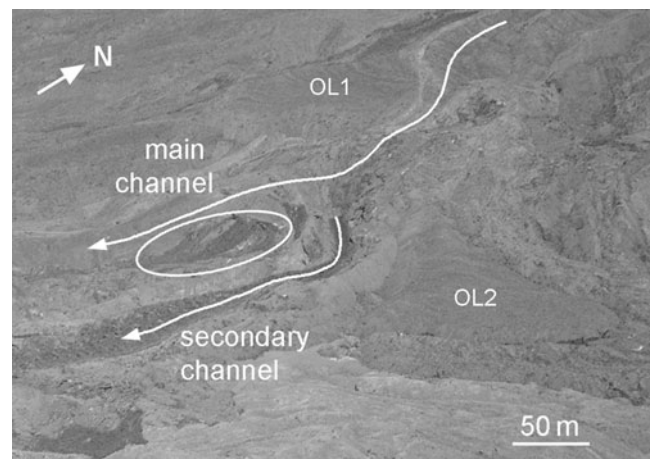


**Fig. 7** Post-eruption image of the Monte Nero breach site from the south east (similar aspect to Fig. 6; the section of flow shown is approximately 500 m long.). The routes of the main (MC) and secondary (SC) channels are shown. The breakout of high-strength lava that occurred on August 3rd is circled, and is much darker than the surrounding 'a'ā. The last material to be emplaced in the secondary channel is also dark in colour

on August 3rd (Fig. 5c), is the subject of the remainder of this paper. These provide valuable insight into the flow dynamics and lava rheology at the time of their formation.

### Late-stage ‘squeeze-up’ extrusions

The processes associated with the opening of ephemeral boccas, and the morphologies of their subsequent products, are well documented (e.g. Rowland and Walker 1987; Jurado-Chichay and Rowland 1995; Dragoni and Tallarico 1996; Calvari and Pinkerton 1998; Polacci and Papale 1999; Sheth et al. 2009). The latest stages of bocca activity in the lower flow field commonly involved the very slow extrusion of high yield strength lava. New, late-stage boccas also formed, extruding similar material as changing flow conditions pressurised parts of the flow that had been stationary for some time (Applegarth 2008). The new boccas opened due to one of two processes. Firstly, the continued or resumed supply of lava along an earlier flow path could result in inflation and carapace failure (Hon et al. 1994; Dragoni and Tallarico 1996; Mattsson and Vuorinen 2008). Alternatively, the ‘toothpaste mechanism’, resulting from late-stage flow superposition and consequent pressurisation of the underlying flow, could lead to crustal rupture and the birth of a new bocca (Applegarth 2008). The name of the mechanism derives from the fact that progressive pressurisation of a flow lobe by an overlying unit is similar to the squeezing of toothpaste from a tube, and does not refer to the resultant extrusion, which may or may not be the toothpaste lava of Rowland and Walker (1987).

Macdonald (1972), citing Nichols (1939), used the term ‘squeeze-up’ to describe surface features ranging from elongate bulbous ridges to sharp pointed wedges, resulting from upwelling through pāhoehoe lava crusts on Hawai‘i (see also Rowland and Walker 1987; Hon et al. 1994; Harris et al. 2009; Sheth et al. 2009). Such features have been described on Etnean slab-crust flows by Guest and Stofan (2005), where they consist of toes or several metres long rolls of pāhoehoe-like lava. Squeeze-ups can also form on high silica flows and domes, forming crease structures (Anderson and Fink 1990, 1992) or spines (Blake 1990). These morphological variations illustrate the need to define whether ‘squeeze-up’ is used to refer to the process or the product. We use the term to describe lava that was extruded from a flow unit at a late stage of (or after) emplacement, and which is easily distinguished from mature rubbly ‘a`ā on all scales. Figure 7 shows that squeeze-ups are much darker in colour than mature ‘a`ā, a feature also noted by Guest and Stofan (2005), which allows them to be identified in aerial images. Fragmentation of squeeze-ups usually results in flattened ‘blades’ of lava rather than relatively equant, ‘a`ā-like clinker.

Bocca formation in flow fronts on Etna occurs on timescales of hours to days (Pinkerton and Sparks 1976), given steady lava supply. If supply is unsteady, or a new surface flow is superposed on an earlier unit after an interval of a few days, the front of the earlier flow may have cooled sufficiently in the interim to resist breaching (Applegarth 2008). In this case, pressurisation of the flow interior may instead cause failure somewhere upstream of the flow front, through a weaker part of the carapace. The loci of squeeze-ups can therefore provide information about the flow rheology beneath the clinker cover. In the lower flow field, squeeze-ups were observed along channel-levée boundaries, which are classic areas of weakness due to shearing of the surface crust, and through flow surfaces behind fronts and within channels. Their occurrence at the centre of channels, where the crust should be most coherent, suggests that pre-existing crustal weaknesses may play a role in determining squeeze-up locations. Squeeze-up morphologies were highly variable, depending on the lava’s rheology and hence its ability to flow away from the bocca upon extrusion. We divide squeeze-ups into ‘flows’, ‘tumuli’ and ‘spines’, the specific features of which are discussed below.

### Flows

Rheological variability resulted in many different surface textures being observed on flows erupted from ephemeral boccas in the lower flow field. Relatively fluid lava produced smooth flows, while higher yield strengths led to toothpaste textures (Rowland and Walker 1987) at low strain rates.

With increasing yield strength, squeeze-up flows developed. These reached up to 250 m in length (Online Resource 1), and often consisted of an unfragmented central zone flanked by clinkery lateral zones, then levées. This is the characteristic structure of flows from ephemeral boccas on Etna (Polacci and Papale 1997, 1999; Guest and Stofan 2005). Figure 8a shows the post-eruption morphology of a flow whose central zone is covered in ‘blade’-like protrusions of lava. The absence of ‘a`ā-like fragmentation suggests that this zone behaved as a plug. The fracture separating the central and lateral zones may be a consequence of the high strength of the lava upon extrusion, or may reflect post-emplacement inflation.

As the yield strength and/or strain rate increased, fragmentation of the flow occurred shortly after extrusion. In the example shown in Fig. 8b the surface of the proximal flow was ‘torn’ transverse to flow direction. Similar morphology was observed by Sheth et al. (2009) in lavas on Barren Island (India), who considered their examples to represent a form of toothpaste lava. In the example shown in Fig. 8a, large-scale fragmentation of the surface occurred approximately two metres downflow of the bocca, producing flattened lava blades. The morphology of these differs



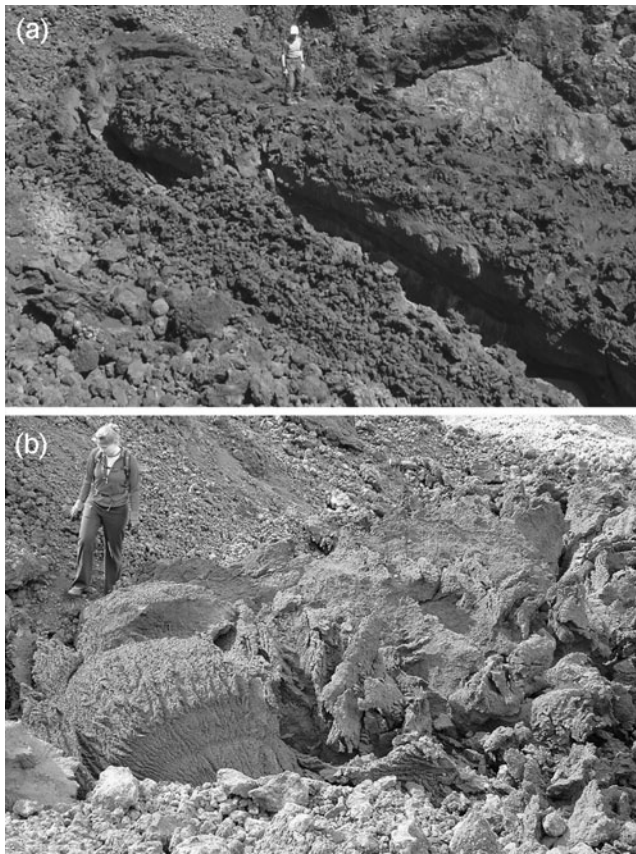


**Fig. 8** Squeeze-up flows. **a** Post-eruption image of the ephemeral bocca that fed the secondary and Monte Grosso channels (upflow end of secondary channel arrow in Figs. 6 & 7). The flow is divided into central and lateral zones by longitudinal fractures. The central zone is covered in blade-like protrusions of lava, indicative of a high yield strength and a low strain rate. **b** Flow that fragmented on a large scale within 2 m of the source bocca, producing flattened blades of lava. Either the lava strength, strain rate or both are therefore inferred to be higher than for the flow in (a). Note that the squeeze-up fragments are markedly different in shape and size from the ‘a`ā clinkers in the foreground

markedly from that of the surrounding ‘a`ā clinkers, which are roughly equant. The curved and twisted blades form a layer ~1 m deep, below which the flow remained coherent. Despite its evident strength, the lava advanced a few tens of metres before halting.

Although lava was extruded in a highly plastic state in the above examples, activity ceased while the material could still ‘flow’ away from the bocca. We next consider the cases in which this was not possible.

#### ‘Tumuli’

*Morphology and relationship to other surface features* In several cases, the bocca supplying a squeeze-up could not be seen because lava had accumulated above the opening. We describe these piles of lava as ‘tumuli’ because of their positive relief, but they differ morphologically from the

smooth-surfaced inflationary structures previously described in both pāhoehoe and ‘a`ā lavas (e.g. Guest et al. 1980; Walker 1991; Rossi and Gudmundsson 1996; Calvari and Pinkerton 1999; Duncan et al. 2004).

The lower flow field tumuli are dome-shaped or elongate in plan view, reaching heights of ~5 m and lengths/diameters of ~20 m, and consist of chaotic arrangements of many lava sheets (Fig. 9a). These sheets are similar in shape to fragmental lava blades, but larger (up to a few metres long/high) in scale. They usually thin towards their extremities, which can be curved and torn (Fig. 9b). The tumuli commonly display a wide central cleft (Fig. 9c), though cleft formation is not ubiquitous. On a large scale, morphological similarities are seen between the lower flow field tumuli and surface features documented elsewhere. For example, tumuli as described on Hawaiian pāhoehoe by Walker (1991), are equant or elongate ‘whale-back shaped’ structures with pervasive surface fractures. Such axial clefts, which are most pronounced in elongate tumuli (Walker 1991), have been observed on tumuli in flows of all compositions (e.g. Mattsson and Vuorinen 2008). The crease structures described in high silica lavas by Anderson and Fink (1990, 1992) are fractures with smoothly convex walls originating from a linear cleft that grow by cyclic fracturing during inflation. Both axial clefts and crease structures develop during inflation-related extension, and provide clues to the growth mechanisms of the lower flow field tumuli.

The sheet-like lava morphology suggests that the source bocca was akin to an inflation cleft, in which case these tumuli could be considered primarily ‘exogenous’ features, as opposed to the ‘endogenous’ tumuli of e.g. Walker (1991), described above. Although endogenous tumuli often have associated extrusions (e.g. Rossi and Gudmundsson 1996; Mattsson and Vuorinen 2008), their overall morphology is governed by the underlying inflation structure, whereas the squeeze-up extrusions dominate the morphology of exogenous tumuli.

*Growth* The lower flow field tumuli often overlie the source areas of squeeze-up flows, suggesting that they represent the latest stages of bocca activity. As activity in the flow field waned, the transport time for lava travelling from the main vent to ephemeral boccas increased. The consequent increase in cooling, degassing and crystallisation led to higher yield strengths. These processes resulted in the last lava to be extruded having a very high yield strength, as evidenced by the juxtaposition of well-defined sheets that are often almost vertical (Fig. 9c).

The laterally extensive sheets arranged around a central cleft suggest that the extrusion of exogenous tumuli took place through openings that were closer to inflation clefts than to the arcuate boccas commonly seen on Etna (Kilburn 1990). We suggest that as supply waned and yield strengths

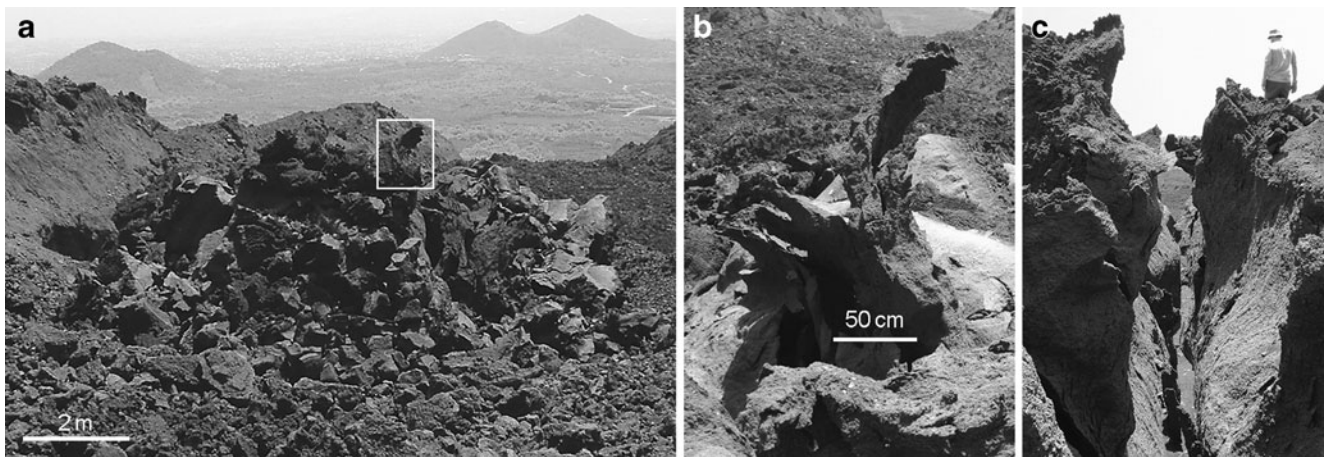


**Fig. 9** Tumulus morphology. **a** Equant, dome-shaped tumulus, which is roughly circular in plan view (diameter ~10 m), and situated in the centre of a channel. Note the chaotic arrangement of lava sheets. **b** Close up of *box* in (a), showing detail of the lava sheets. These thin

towards their extremities, folding and tearing. **c** Looking down the central cleft of an elongate tumulus. The central pair of lava sheets extend laterally for ~15 m, and vertically for ~3 m. On either side of this pair, the lava sheets are again randomly oriented

increased, the arcuate boccas that had previously supplied relatively fluid flows began to extrude first toothpaste then squeeze-up flows. Eventually, the strength of the lava prevented it from being extruded under gravity, and the boccas became blocked. Continued supply then caused overpressure and inflation, producing endogenous tumuli that subsequently failed in a brittle manner to form inflation clefts through which the highly plastic lava was extruded. The lava's yield strength prevented it from flowing away upon extrusion, so that it accumulated over the cleft, resulting in exogenous tumulus growth.

The reason for the chaotic arrangement of lava sheets is unclear. It is possible that, following the emplacement of a central pair of sheets from an inflation cleft, further squeeze-ups developed from the same fracture. Alternatively, pervasive fracturing of the carapace (Walker 1991) may have allowed many sheets to develop simultaneously. Krauskopf (1948) described 'curved slabs' of lava on flows and around fissures at Parícutin (Mexico) which are similar in morphology to the lava sheets. He witnessed the growth of these slabs from fissures and invoked the same mechanism for their development on the flows. He described how 'lava is pushed up slowly from beneath, splitting into slabs as it cools and contracts; then each slab grows as it is pushed outward, plastic at its base but cold and hard in its upper part'. The cleaving of sheets may have occurred during early tumulus growth on Etna, but the overall chaotic distribution suggests that more than one squeeze-up phase occurred at one or more source fractures.

**Succession** The height of an endogenous tumulus is a function of the internal magmatic overpressure and the flexural rigidity of the surface crust, which itself depends on the crustal thickness (Rossi and Gudmundsson 1996).

As a tumulus grows, the magmastatic head decreases, eventually preventing further growth. A similar feedback may operate in exogenous tumuli. Once growth ceases, continued supply to the area may cause sufficient overpressure to initiate a new tumulus nearby. This mechanism is inferred in the development of three closely-spaced tumuli that grew during the latter stages of activity, in the right hand arm of the distal main channel adjacent to Monte Concilio. These tumuli (identified by the long arrow in Online Resource 1) are aligned down a 50 m section of the channel. The lowest (furthest downslope) of the three tumuli displays exogenous morphology, and is associated with a squeeze-up flow ~150 m in length. The middle tumulus occurs with a 20 m long flow, and although largely made up of lava sheets, is underlain by a smooth-surfaced bulge in the channel. The upper tumulus is entirely endogenous, with a central cleft, and occurs with a 10 m long flow (Fig. 10).

We consider that the lowest bocca developed first. Following the emplacement of the long flow, waning supply resulted in blockage of the bocca as the lava was too plastic to flow. Continued supply to the area produced an overpressure that caused inflation, crustal failure and the emplacement of the exogenous tumulus. As the tumulus grew, the magmastatic head decreased, eventually preventing further extrusion and again blocking the subsurface pathway. Because lava continued to be supplied to the area, the pressure in the pathway increased once more and resulted in a second bocca, above the blockage. In this case, probably due to the reduced magmastatic head, only a short flow was emplaced before the bocca became blocked and tumulus growth began. The tumulus was also smaller as a result of the reduced head, and insufficient lava was extruded to completely mask the initial endogenous tumulus.

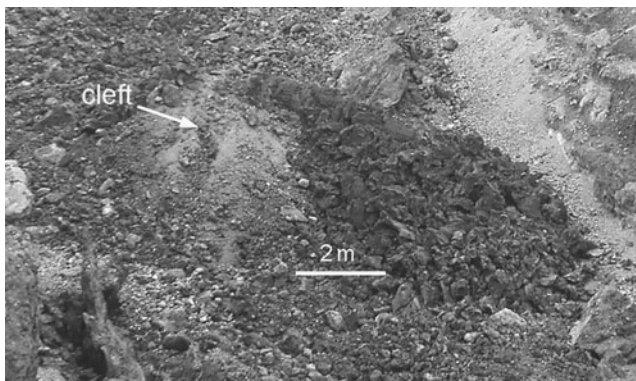


**Fig. 10** The upper tumulus in a trio inferred to have grown successively upflow, the lower and middle of which are similar in morphology to that shown in Fig. 9a. The tumulus pictured, which is ~6 m in diameter, fed a short, fragmented flow, seen on the right of this image, but has no associated bladed lava sheets. Instead, the flow surface is domed upwards, demonstrating endogenous morphology. What may be an incipient central cleft is indicated. This may have been exploited by a squeeze-up had activity continued

Cessation of activity in this locality again led to repetition of the process upslope where, following emplacement of the shortest flow, overpressure was only sufficient to produce an endogenous tumulus.

The upper tumulus is considerably narrower than the underlying flow surface (Fig. 10), suggesting that the subsurface thermal pathway was narrower than earlier active flows. The reduced volume of material extruded by successive boccas also reflects the waning effusion rates during the late stages of the eruption.

### Spines

In the extreme end-member case, lava that is near-solid can be extruded to form spines. Spines are common on high silica lava domes (Blake 1990) and blocky lava flows (Macdonald 1972), but are comparatively rare on basaltic `a`ā flows. In the lower flow field, spines formed in the region immediately behind the flow front. Spine formation can sometimes be linked to the process of ‘ramping’ (e.g. Christiansen and Lipman 1966), whereby movement on internal shear planes behind a congealing front occurs in an upward rather than a forward direction (Macdonald 1972; Rowland and Walker 1990). Ramping often results in small hillocks in the flow surface. Hillocks were observed in conjunction with spines behind the front of the lower flow field (Fig. 11a), supporting the idea that ramping occurred in this flow.

### Other morphological variants

In some cases, the latter stages of activity of a bocca resulted not in bladed tumuli, but in mounds of massive

lava. Elsewhere, groups of lava sheets similar in morphology to the tumuli were observed on a range of scales, but without associated earlier flows (Fig. 11b). The precise morphology that develops is probably a function of the lava rheology and the extrusion (and hence strain) rate (Kilburn 1990), as well as the volume of lava available for extrusion and the bocca geometry. Figure 12 provides a schematic indication of the morphology that might be expected under differing conditions. The shape of the pāhoehoe-`a`ā transition was proposed by Peterson and Tilling (1980) and refined by Kilburn (1981), who envisaged a diffuse ‘transition threshold zone’ (TTZ) between the two morphological fields rather than a sharp boundary. We suggest that a further boundary, between `a`ā and bladed flows, would have a similar shape. The low strain rate-high viscosity morphologies are shown in the relevant region of the plot, but shapes of these boundaries are somewhat arbitrary.

### Small-scale surface textures

Lava extruded as squeeze-up flows and tumuli was often observed to have torn on a large scale upon extrusion (Figs. 8b, 9b). Smaller-scale platy cleaving also occurred as the blades and sheets folded over (Fig. 13). This morphology indicates that although the interior of the sheet was

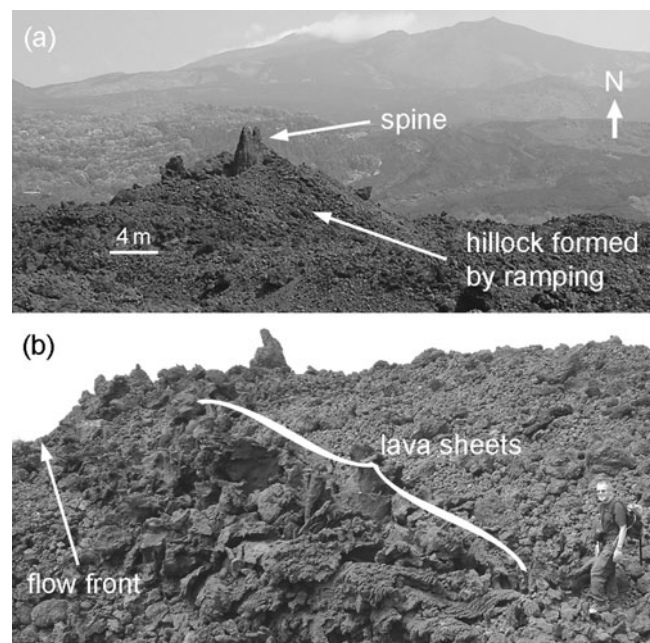


**Fig. 11** **a** Hillocks and spines a few hundred metres behind the flow front, which resulted from upward ramping on internal shear planes in the flow, as the stagnating front could no longer advance forwards. The spine is approximately 4 m in height, and the hillock 20 m in diameter. **b** Squeeze-up lava sheets, similar in form to the tumuli sheets, but without an associated earlier flow. This example occurs within a few tens of metres of the flow front, the upper part of which can be seen to the left of the image

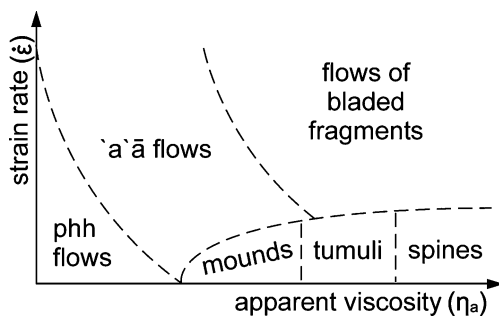


**Fig. 12** Schematic representation of squeeze-up morphology as a function of the apparent viscosity,  $\eta_a$ , and the strain rate,  $\dot{\epsilon}$ , to which the lava is subjected. If the lava is assumed to behave as a Bingham fluid, the use of apparent viscosity can take into account the effects of both the Bingham viscosity and the yield strength (Kilburn 1981). At low  $\eta_a$ , long, coherent pāhoehoe (phh) flows form, even at high  $\dot{\epsilon}$ . As  $\eta_a$  increases, fragmentation occurs at high  $\dot{\epsilon}$ , while at low  $\dot{\epsilon}$ , lava accumulates over the bocca, producing variably mounds, tumuli or spines. Although the boundaries between the fields are shown as lines, they are more likely to be wide, diffuse regions, like the ‘transition threshold zone’ (TTZ) between pāhoehoe and `a`ā fields in the strain rate-viscosity diagrams of Peterson and Tilling (1980), or the family of ‘fluidity flow curves’ used by Kilburn (1981) to represent the TTZ in strain rate-apparent viscosity space

behaving in a ductile manner, the outer layers were undergoing brittle deformation. Where squeeze-up lava was extruded in a near-solid state, friction between the squeeze-up and the flow carapace produced fine-grained gouge that was red or white in colour.

## Discussion

### Squeeze-up morphologies

The surface textures and morphologies of late-stage squeeze-ups in the lower flow field differ markedly from those of the `a`ā that accounts for most of the flow field. Our observations lead us to propose an alternative interpretation for the formation of the most advanced flow front lobe of the lower flow field (arrow, Fig. 14a) to that offered by Favalli et al. (2010). We also suggest a different model for the latest stages of flow front advance as a whole.

Favalli et al. (2010) suggest that the flow front advanced as a series of lobes moving forwards one at a time, rather than as a single unit. The lobes are thought to have originated as breakouts of low-yield-strength lava from the core of the stalled flow front, which then subsequently inflated. They interpret the most advanced unit as a failed lobe that would have inflated to resemble the other lobes had activity not been waning, inferring a low yield strength from the fact that it is anomalously thin, and calculating its yield strength from its thickness, assuming Bingham behaviour.

We propose instead that the overall lobate structure of the flow front may have developed because of crustal heterogeneities that arose due to shear fracturing of the crust as lateral spreading occurred in the zone of dispersed flow. This process has been observed in analogue models in which a ductile core is directly overlain by a brittle crust (Applegarth 2008). We suggest that the presence of lobes does not necessarily indicate that breaching of the carapace has occurred. It is therefore possible that the flow front lobes developed (and advanced) contemporaneously rather than one at a time. In this scenario, the anomalously thin central lobe requires a different explanation.

We observed that the central lobe is darker in colour than the surrounding lobes (Fig. 14a) and that its surface is covered by a significant proportion of bladed lava sheets (Fig. 14b), though `a`ā clinker is also present. This is in agreement with the observation of Favalli et al. (2010) that the lobe has a blockier crust than the other flow front lobes, and extensive ooze-outs of spiny toothpaste pāhoehoe. The surface texture of this lobe, and the extensive presence of squeeze-up extrusions on the near sides of the adjacent flow front lobes (Fig. 11b), lead us to suggest that it may be a late-stage squeeze-up flow rather than a low viscosity extrusion as inferred by Favalli et al. (2010). However, the issue of its lower thickness in comparison to the adjacent lobes does seem to favour the low viscosity hypothesis (Fig. 14a).

During our examination of the flow front region we observed several laterally extensive (several tens of metres), highly fragmented squeeze-up flows emerging from the flow margins (Online Resource 1). These are similar in form to the central lobe, but not as closely associated with loci of earlier lobe advance. In all cases, these were



**Fig. 13** ‘Peeling’ textures on the surface of a lava sheet indicate brittle deformation of the outer layer, while the curvature of the sheet shows that the core is still sufficiently ductile to fold under its own weight

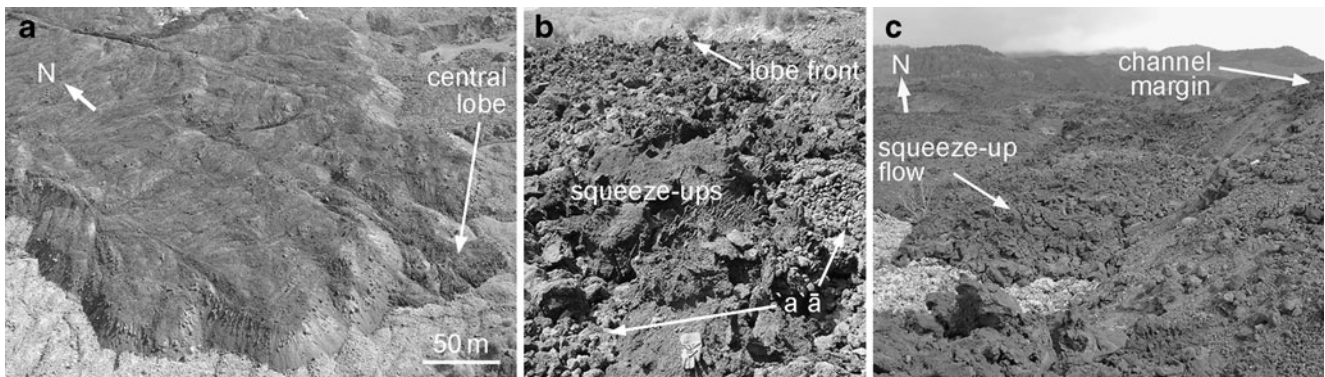


**Fig. 14** **a** The 2001 flow front, illustrating the similarity in shape, size and colour of the thicker, older frontal lobes. The flow front is 200–300 m wide in this image. The arrow indicates the most advanced lobe, interpreted by Favalli et al. (2010) as a failed lobe of lower yield strength lava, because it is thinner than the adjacent lobes. This lobe is darker than the surrounding a'ā. **b** Close up of the surface of the lobe

identified in (a), showing bladed squeeze-ups and a'ā clinker. Note glove for scale. **c** Another squeeze-up flow observed to the east of the flow field, approximately 500 m behind the flow front. This flow is made up of bladed fragments, indicative of a high yield strength, yet is significantly thinner (~5 m) than the adjacent transitional channel (~15 m). The front of the squeeze-up flow is approximately 15 m wide

significantly thinner than the main body of the flow, being in general less than 5 m thick (Fig. 14c), compared to 15 to 30 m for the larger flow front lobes and the transitional channel up to 800 m behind the flow front (Favalli et al. 2010). Because these features are morphologically similar to the most advanced lobe, we argue that they are all of the same origin. We favour their interpretation as late-stage squeeze-up flows rather than failed lobes.

We therefore suggest that lava flow textures and histories should be examined on a case by case basis to ensure that the assumption of Bingham rheology can be confidently applied, as we feel that thickness alone cannot always be used to differentiate between the rheologies of different flows. In the case of the lower flow field, the main flow front lobes may have undergone post-emplacment inflation, while the squeeze-up flows probably have not, and may even have advanced in a manner more akin to that of blocky flows.

#### Core vs. Crustal control on tumulus development

Exogenous tumuli differ in morphology from their endogenous counterparts, reflecting both a significant rheological contrast and the relative importance of the flow core and surface crust at the time of formation. Endogenous tumuli generally form in regions of shallowing local slope, where lava supply exceeds drainage (e.g. Duncan et al. 2004). The resulting inflation causes upward flexure of the surface crust (ductile deformation), and subsequent failure, resulting in inflation clefts (brittle deformation). In this case, tumulus location and growth are predominantly controlled by the magmatic head in the flow core, as the resistance of the crust is minimal.

Exogenous tumuli in the lower flow field are also strongly dependent on overpressure in the flow core, as the extrusion of lava with a very high yield strength

requires a significant pressure gradient. However, when they occur in the channel centre (as opposed to at channel-levee boundaries), this is often in regions of steep or increasing local slope. This suggests that their formation is also strongly influenced by the state of the surface crust. Slope angles for the main channel are given in Online Resource 1, though localised changes, which may still have a significant influence, are not resolvable at this scale. Because the tumuli are late-stage features, cooling and thickening of the crust is likely to have resulted in a significant flexural rigidity (Rossi and Gudmundsson 1996). Very high overpressures in the flow interior would therefore have been required to deform the crust where it is coherent, and tumulus location may instead be controlled by pre-existing weaknesses in the crust. Field observations (Macdonald 1972; Kilburn 1990; Crisp and Baloga 1994) and analogue experiments (Applegarth 2008) indicate that surface crusts are often disrupted by the action of tensile stresses in regions where the flow accelerates, such as increases in the local slope. Failure of the crust earlier in the flow history could have resulted in fractures that were later exploited as overpressures developed in the flow interior.

We suggest that the prevailing flow conditions determine whether a tumulus develops with either predominantly endogenous or exogenous morphology. A transition from endogenous to exogenous morphology would be expected as activity progresses, representing a shift from core- to crust-controlled dynamics.

#### Flow textures, rheology and implications for hazard assessment

When modelling lava flows, the conditions under which a flow will no longer be able to advance must be defined. Although the cessation of flow is thought to occur at a

critical crystallinity (e.g. Marsh 1981; Lejeune and Richet 1995; Pinkerton and Stevenson 1992), this value is not yet known. The exogenous tumuli in the lower flow field display morphologies that suggest they are approaching the most advanced state in which lava can ‘flow’, which may perhaps reflect a crystallinity that is approaching the critical threshold. If this is the case, studying the texture and behaviour of tumuli may have implications for rheological studies and modelling.

Although unlikely to advance under gravity alone, tumulus material was able to ‘flow’ due to high overpressures in the flow interior. The curved slabs described by Krauskopf (1948) on Parícutin made up the entire lower half of the 10 km long basaltic San Juan Parangaricutiro flow. Krauskopf examined this flow after the eruption, but its emplacement was observed by Foshag and Gonzalez-Reyna (account from Luhr and Simkin 1993) who described its interrupted advance over several months. Six months after its initiation, following a 1 month pause in advance, tongues of ‘highly plastic’ lava broke out from the flow front. Several days later, streams of more fluid lava appeared at the front, and advanced rapidly to cover an area of 350,000 m<sup>2</sup> in one night. The initial plastic lava tongues, which correspond to Krauskopf’s curved slabs, are inferred to result from the enforced drainage of the pressurised flow interior. Observations of the drainage indicate that the plastic lava tongues were each active for less than 1 day, but attained advance rates of up to 40 m hr<sup>-1</sup> (Luhr and Simkin 1993).

The San Juan flow was fed by a vent supplying lava to several flows that were active contemporaneously, and was subject to pulses in supply as the locus of activity changed. Between pulses, cooling and degassing led to the stagnation of the flow. When supply resumed, however, it was able to force drainage of the flow front by the transmission of fluid pressure along the earlier flow path. Once the plastic lava had been drained to form a tube system, a large volume of fresh lava was emplaced over a short time.

### Degassing

Krauskopf (1948) reported that the curved slabs on the San Juan flow had ‘normal’ temperatures, but ‘abnormally low’ gas contents (although he took no direct measurements). If the gas content was indeed low, the observed high lava strength may have arisen from crystal growth as a result of degassing-related undercooling (e.g. Sparks and Pinkerton 1978; Cashman and Blundy 2000), without the need for significant surface cooling. Petrographic examination of the 2001 squeeze-up lava may provide insights into degassing processes, which are not currently understood sufficiently to be incorporated into flow models.

### Conclusions

Most long-lived basaltic eruptions produce compound products that include a wide range of features formed at different times during the activity, and which are challenging to interpret. Although the 2001 eruption of Etna lasted for just 23 days, it produced an excellent example of a compound ‘a’ flow field.

The final large-scale morphology of the lower flow field depended on many factors, including effusion rate. Small, transient changes in this parameter during the late eruption were observed to have a major influence on the structure of the lower flow field. They caused overflows and surface flows, and contributed to levée breaching, though other factors such as the stagnation and ponding of flow units within channels also influenced breaching events. Ponding occurs in regions of shallowing slope, so topography played a significant role in determining where the Monte Nero and Monte Grosso breaches occurred. A transient increase in effusion rate can amplify the topographically controlled effects of ponding, as can the development of blockages downflow (e.g. Lipman and Banks 1987; Harris et al. 2009). Both breaches occurred on the outside of channel bends.

The apparent correlation between small changes in effusion rate and significant morphological changes in the lower flow field highlights the need to monitor the effects of effusion rate changes throughout flow fields. The simultaneous vent and flow field observations required to link morphological changes to effusion rate variations with confidence places a considerable strain on resources during long-lived eruptions, but may improve our ability to forecast apparently stochastic processes. The accurate prediction of such events in both time and space is unlikely to be possible within numerical flow models. However, factors such as topography and channel geometry could be used as preliminary predictive tools when attempting to forecast where breaches may occur. Linking these factors to observed changes at the vent and precursory events, such as overflows and evidence of levée destabilisation (Favalli et al. 2010), may also allow the timing of such events to be estimated. Monitoring the progress and stagnation of flow units may also enable sites of ephemeral bocca formation to be anticipated. Following the identification of possible sites of breaching or bocca formation in active flows, these could be used as the starting points for the simulation of new flows, to assess their possible consequences. The importance of such assessments was illustrated by the sudden 40° change in direction of flow field advance following the initiation of the Monte Grosso channel (Fig. 2), which could have had severe hazard implications in a more developed area. We suggest that measuring effusion rates close to the vent is the most effective way of gaining

possible predictive advantage. During future eruptions, the use of long range laser scanners to obtain sequential DEMs may provide an improved method of addressing this problem (James et al. 2009).

Our observations of the development of the lower flow field have implications for the assessment of potential hazards during future eruptions on Etna and other volcanoes. The widespread reactivation of cooled flow units due to the influence of later flows could represent a serious potential hazard, either due to the remobilisation of large volumes of previously stationary lava, which could follow a different path to the original flow, or through the forced drainage of stationary flows to produce a tube system that would significantly increase the distance lava could travel from the vent (e.g. Keszthelyi 1995; Thordarson and Self 1998; Calvari and Pinkerton 1998).

Long-lived, tube-fed compound flow fields are known from many of Etna's previous eruptions (e.g. Pinkerton and Sparks 1976; Calvari and Pinkerton 1998, 1999), as well as elsewhere (e.g. Mattox et al. 1993; Keszthelyi and Self 1998) but there is no precedent on Etna for large-scale reactivation of a flow front following such a long period of inactivity as seen at Parícutin. Examples from other volcanoes are also lacking. Nonetheless, the widespread distribution of small, highly viscous squeeze-ups on Etna, as well as Hawai'i (e.g. Harris et al. 2009) and Barren Island (Sheth et al. 2009), indicates that late-stage core remobilisation is possible and we therefore suggest that the possibility should not be discounted.

**Acknowledgements** We thank INGV Catania for providing the images used in our study. Reviews by Angus Duncan and one anonymous reviewer greatly improved this manuscript. The work was funded by Natural Environment Research Council studentship NER/S/A2005/13681 and grant NE/F018010/1. MRJ was funded by the Royal Society.

## References

- Anderson SW, Fink JH (1990) The development and distribution of surface textures at the Mount St-Helens dome. In: Fink JH (ed) *Lava flows and domes*. Springer, Berlin, pp 25–46
- Anderson SW, Fink JH (1992) Crease structures—indicators of emplacement rates and surface stress regimes of lava flows. *Geol Soc Am Bull* 104:615–625
- Applegarth LJ (2008) Complexity in lava flows: surface features and structural morphology, PhD thesis, Lancaster University
- Bailey JE, Harris AJL, Dehn J, Calvari S, Rowland S (2006) The changing morphology of an open lava channel on Mt. Etna. *Bull Volcanol* 68:497–515
- Behncke B, Neri M (2003) The July–August 2001 eruption of Mt. Etna (Sicily). *Bull Volcanol* 65:461–476
- Blake S (1990) Viscoplastic models of lava domes. In: Fink JH (ed) *Lava flows and domes*. Springer, Berlin, pp 88–126
- Borgia A, Linneman S, Spencer D, Morales LD, Andre JB (1983) Dynamics of lava flow fronts, Arenal-Volcano, Costa Rica. *J Volcanol Geotherm Res* 19:303–329
- Calvari S, Pinkerton H (1998) Formation of lava tubes and extensive flow field during the 1991–1993 eruption of Mount Etna. *J Geophys Res* 103:27291–27301
- Calvari S, Pinkerton H (1999) Lava tube morphology on Etna and evidence for lava flow emplacement mechanisms. *J Volcanol Geotherm Res* 90:263–280
- Calvari S, INGV Catania staff (2001) Multidisciplinary approach yields insight into Mt. Etna 2001 eruption. *EOS Trans AGU* 82(52):653–656
- Calvari S, Pinkerton H (2004) Birth, growth and morphologic evolution of the “Laghetto” cinder cone during the 2001 Etna eruption. *J Volcanol Geotherm Res* 132:225–239. doi:10.1016/S0377-0273(03)00347-0
- Calvari S, Neri M, Pinkerton H (2003) Effusion rate estimations during the 1999 summit eruption on Mount Etna, and growth of two distinct lava flow fields. *J Volcanol Geotherm Res* 119:107–123. doi:10.1016/S0377-0273(02)00308-6
- Cashman KV, Blundy J (2000) Degassing and crystallisation of ascending andesite and dacite. *Phil Trans Roy Soc London* 358:1487–1513
- Chester DK, Duncan AM, Guest JE, Kilburn CRJ (1985) Mount Etna: the anatomy of a volcano. Chapman and Hall, London
- Christiansen R, Lipman PW (1966) Emplacement and thermal history of a rhyolite lava flow near Fortymile Canyon, southern Nevada. *Geol Soc Am Bull* 77:671–684
- Coltelli M, Proietti C, Branca S, Marsella M, Andronico D, Lodato L (2007) Analysis of the 2001 lava flow eruption of Mt. Etna from three-dimensional mapping. *J Geophys Res* 112:F02029. doi:10.1029/2006JF000598
- Crisci G, Rongo R, Gregorio S, Spataro W (2004) The simulation model SCiARA: the 1991 and 2001 lava flows at Mount Etna. *J Volcanol Geotherm Res* 132:253–267
- Crisp J, Baloga S (1994) Influence of crystallisation and entrainment of cooler material on the emplacement of basaltic aa lava flows. *J Geophys Res* 99:11819–11831
- Dragoni M, Tallarico A (1996) A model for the opening of ephemeral vents in a stationary lava flow. *J Volcanol Geotherm Res* 74:39–47
- Duncan AM, Guest JE, Stofan ER, Anderson SW, Pinkerton H, Calvari S (2004) Development of tumuli in the medial portion of the 1983 'a'ā flow-field, Mount Etna, Sicily. *J Volcanol Geotherm Res* 132:173–187
- Favalli M, Pareschi M, Neri A, Isola I (2005) Forecasting lava flow paths by a stochastic approach. *Geophys Res Lett* 32:L03305. doi:10.1029/2004GL021718
- Favalli M, Harris AJL, Fornaciai A, Pareschi MT, Mazzarini F (2010) The distal segment of Etna's 2001 basaltic lava channel. *Bull Volcanol* 72:119–127. doi:10.1007/s00445-009-0300-z
- Frazzetta G, Romano R (1984) The 1983 Etna eruption: event chronology and morphological evolution of the lava flow. *Bull Volcanol* 47:1079–1096
- Guest JE, Stofan ER (2005) The significance of slab-crust lava flows for understanding controls on flow emplacement at Mount Etna, Sicily. *J Volcanol Geotherm Res* 142:193–205
- Guest JE, Underwood JR, Greeley R (1980) Role of lava tubes in flows from the observatory-vent, 1971 eruption on Mount Etna. *Geol Mag* 117:601–606
- Guest JE, Kilburn CRJ, Pinkerton H, Duncan AM (1987) The evolution of lava flow-fields: observations of the 1981 and 1983 eruptions of Mount Etna, Sicily. *Bull Volcanol* 49:527–540
- Harris AJL, Rowland SK (2001) FLOWGO: a kinematic thermo-rheological model for lava flowing in a channel. *Bull Volcanol* 63:20–44
- Harris AJL, Dehn J, Calvari S (2007) Lava effusion rate definition and measurement: a review. *Bull Volcanol* 70:1–22

- Harris AJL, Favalli M, Mazzarini F, Hamilton CW (2009) Construction dynamics of a lava channel. *Bull Volcanol* 71:459–474. doi:10.1007/s00445-008-0238-6
- Hidaka M, Goto A, Umino S, Fujita E (2005) VTFS project: Development of the lava flow simulation code LavaSIM with a model for three-dimensional convection, spreading, and solidification. *Geochem Geophys Geosys* 6:Q07008. doi:10.1029/2004GC000869
- Hon K, Kauahikaua J, Denlinger R, Mackay K (1994) Emplacement and inflation of pāhoehoe sheet flows- observations and measurements of active lava flows on Kilauea Volcano, Hawai'i. *Geol Soc Am Bull* 106:351–370
- Istituto Nazionale di Geofisica e Vulcanologia (Catania) syn-eruption reports: <http://www.ct.ingv.it/Etna2001/Main.htm>
- James MR, Pinkerton H, Robson S (2007) Image-based measurement of flux variation in distal regions of active lava flows. *Geochem Geophys Geosys* 8:Q03006. doi:10.1029/2006GC001448
- James MR, Pinkerton H, Applegarth LJ (2009) Detecting the development of active lava flow fields with a very-long-range terrestrial laser scanner and thermal imagery. *Geophys Res Lett* 36:L22305. doi:10.1029/2009GL040701
- Jurado-Chichay Z, Rowland SK (1995) Channel overflows of the pohue bay flow, Mauna-Loa, Hawai'i- examples of the contrast between surface and interior lava. *Bull Volcanol* 57:117–126
- Kauahikaua J, Sherrod DR, Cashman KV, Heliker CC, Hon K, Mattox TN, Johnson JA (2003) Hawai'iian lava-flow dynamics during the Pu'u-O'o-Kupaianaha eruption: a tale of two decades. *US Geol Surv* 1676:63–87
- Keszthelyi L (1995) A preliminary thermal budget for lava tubes on the Earth and planets. *J Geophys Res* 100:20411–20420
- Keszthelyi L, Self S (1998) Some physical requirements for the emplacement of long basaltic lava flows. *J Geophys Res* 103:27447–27464
- Kilburn CRJ (1981) Pāhoehoe and 'a'ā-lavas- a discussion and continuation of the model of Peterson and Tilling. *J Volcanol Geotherm Res* 11:373–382
- Kilburn C (1990) Surfaces of 'a'ā flow-fields on Mount Etna, Sicily- morphology, rheology, crystallisation and scaling phenomena. In: Fink JH (ed) *Lava flows and domes*. Springer, Berlin, pp 129–156
- Kilburn CRJ, Lopes RMC (1988) The growth of 'a'ā lava flow-fields on Mount Etna, Sicily. *J Geophys Res* 93:14759–14772
- Kilburn CRJ, Lopes RMC (1991) General patterns of flow field growth- 'a'ā and blocky lavas. *J Geophys Res* 96:19721–19732
- Krauskopf KB (1948) Lava movement at Parícutin volcano, Mexico. *Geol Soc Am Bull* 59:1267–1283
- Lejeune AM, Richet P (1995) Rheology of crystal-bearing silicate melts- an experimental-study at high viscosities. *J Geophys Res* 100:4215–4229
- Lipman PW, Banks NG (1987) 'A'ā flow dynamics, Mauna Loa 1984. *US Geol Surv* 1350:1527–1568
- Luhr JF, Simkin T (1993) Parícutin, the volcano born in a Mexican cornfield. *Geoscience, Arizona*
- Macdonald GA (1972) *Volcanoes*. Prentice-Hall, New Jersey
- Marsh BD (1981) On the crystallinity, probability of occurrence, and rheology of lava and magma. *Contrib Mineral Petrol* 78:85–98
- Mattox TN, Heliker C, Kauahikaua J, Hon K (1993) Development of the 1990 Kalapana flow-field, Kilauea Volcano, Hawai'i. *Bull Volcanol* 55:407–413
- Mattsson HB, Vuorinen J (2008) Emplacement and inflation of natrocarbonatitic lava flows during the March–April 2006 eruption of Oldinyo Lengai, Tanzania. *Bull Volcanol* 71:301–311. doi:10.1007/s00445-008-0224-z
- Mazzarini F, Pareschi MT, Favalli M, Isola I, Tarquini S, Boschi E (2005) Morphology of basaltic lava channels during the Mt. Etna September 2004 eruption from airborne laser altimeter data. *Geophys Res Lett* 32:L04305. doi:10.1029/2004GL021815
- Nichols RN (1939) Squeeze-ups. *J Geol* 47:421–425
- Peterson DW, Tilling RI (1980) Transition of basaltic lava from pāhoehoe to 'a'ā, Kilauea volcano, Hawai'i- field observations and key factors. *J Volcanol Geotherm Res* 7:271–293
- Pinkerton H, Sparks RSJ (1976) 1975 sub-terminal lavas, Mount Etna- case history of formation of a compound lava field. *J Volcanol Geotherm Res* 1:167–182
- Pinkerton H, Stevenson RJ (1992) Methods of determining the rheological properties of magmas at sub-liquidus temperatures. *J Volcanol Geotherm Res* 53:47–66
- Pinkerton H, Wilson L (1994) Factors controlling the lengths of channel-fed lava flows. *Bull Volcanol* 56:108–120
- Polacci M, Papale P (1997) The evolution of lava flows from ephemeral vents at Mount Etna: insights from vesicle distribution and morphological studies. *J Volcanol Geotherm Res* 76:1–17
- Polacci M, Papale P (1999) The development of compound lava fields at Mount Etna. *Phys Chem Earth A—Solid Earth and Geodesy* 24:949–952
- Rossi MJ, Gudmundsson A (1996) The morphology and formation of flow-lobe tumuli on Icelandic shield volcanoes. *J Volcanol Geotherm Res* 72:291–308
- Rowland SK, Walker GPL (1987) Toothpaste lava: characteristics and origin of a lava structural type transitional between pāhoehoe and 'a'ā. *Bull Volcanol* 49:631–641
- Rowland SK, Walker GPL (1990) Pāhoehoe and 'a'ā in Hawai'i: volumetric flow rate controls the lava structure. *Bull Volcanol* 52:615–628. doi:10.1007/BF00301212
- Sheth HC, Ray JS, Bhutani R, Kumar A, Smitha RS (2009) Volcanology and eruptive styles of Barren Island: an active mafic stratovolcano in the Andaman Sea, NE Indian Ocean. *Bull Volcanol* 71:1021–1039. doi:10.1007/s00445-009-0280-z
- Sparks RSJ, Pinkerton H (1978) Effect of degassing on rheology of basaltic lava. *Nature* 276:385–386
- Thordarson T, Self S (1998) The Roza Member, Columbia River Basalt Group: A gigantic pāhoehoe lava flow field formed by endogenous processes? *J Geophys Res* 103:27411–27445
- Vicari A, Herault A, Del Negro C, Coltelli M, Marsella M, Proietti C (2007) Modelling of the 2001 lava flow at Etna volcano by a Cellular Automata approach. *Environ Model Softw* 22:1465–1471
- Walker GPL (1973) Lengths of lava flows. *Phil Trans Roy Soc London A—Math Phys and Eng Sci* 274:107–118
- Walker GPL (1991) Structure, and origin by injection of lava under surface crust, of tumuli, lava rises, lava-rise pits, and lava-inflation clefts in Hawai'i. *Bull Volcanol* 53:546–558
- Wright R, Garbeil H, Harris AJL (2008) Using infrared satellite data to drive a thermo-rheological/stochastic lava flow emplacement model: a method for near-real-time volcanic hazard assessment. *Geophys Res Lett* 35:L19307. doi:10.1029/2008GL035228